

MVA Master Stage Report

Decomposition Operators for the Tone Mapping of High Dynamic Range Images

Cristian Felipe Ocampo Blandón

Research Master Thesis, Master 2 MVA.
2013-2014

Advisor: Yann Gousseau



École Normale
Supérieure de Cachan



Telecom
ParisTech

Acknowledgment

I would like to warmly thank Professor Yann Gousseau for his excellent supervision and his exceptional human qualities. I also would like to thank the whole TSI team at Telecom ParisTech.

Abstract

Along with the popularization of digital cameras, comes an increasing desire for accurately capturing difficult scenes. This implies robustness to strong illumination changes, a situation that conventional cameras are not able to handle. For the purpose of obtaining the true intensities of a scene and offering a sensation of human-like reproduction, HDR imaging was created. The corresponding techniques are capable of reproducing a scene having huge contrasts and illumination changes, both for indoor and outdoor scenarios. However, since the resulting HDR data possesses a high dynamic range, conventional visualization and printing devices are incapable of managing HDR images. The task of reducing the dynamic range without losing visual quality is called tone mapping. Although many efficient methods have been proposed in the field, they are still not perfect and often corrupt the resulting image by altering the quality of details and by including halo artifacts. One classical method is the use of the bilateral filter for tone mapping, yielding the decomposition of the image in two components, large scale (Base) and detail components. For dynamic range reduction, the base component is compressed and subsequently integrated with the detail component. Inspired by this approach to tone mapping, in this document we explore several alternatives for computing the tone mapped image without introducing halo artifact or deteriorating the quality of the resulting image. Particularly, we studied geometry/texture decomposition filters and a particular connected filter derived from the fast level set transform. The results are promising for reducing halo artifact and giving a visually appealing outcome. However, there are still open problems that are likely to be solved following this path.

Contents

Acknowledgment	iii
List of Figures	ix
1 Introduction	1
2 Previous Work	3
3 Algorithms Studied	9
3.1 HDR Compression Methods: Two Classical Methods	9
3.1.1 Gradient Based Approach	9
3.1.2 Base and detail image decomposition by using the bilateral filter . . .	12
3.2 Using Denoising and Geometry/Texture filters for image decomposition . . .	14
3.2.1 Total variation	14
3.2.2 Non local means	15
3.2.3 Cartoon+Texture	16
3.2.4 Cartoon+Texture with the TV-L1	17
3.2.5 Fast level set transform	17
3.2.6 Examples	18
4 Experiments and Results	21
4.1 Implementation for the HDR tone mapping methods	21
4.1.1 Gradient domain compression	21
4.1.2 Bilateral Filter for tone mapping	22
4.2 Dataset and evaluation protocol	22
4.3 Experimental Settings	23
4.4 Results	23
4.5 Analysis	23
5 Conclusions	31
6 Bibliography	33

List of Figures

2-1	Conventional device enabled with HDR capabilities.	3
3-1	Influence function.	17
3-2	(a). House in the field image. Output of the filters for: Total variation - cartoon (b) and texture (c), Nonlocal Means - cartoon (d) and texture (e). .	19
3-3	Output of the filters for: cartoon + texture - cartoon (a) and texture (b). cartoon - texture L1 - cartoon (c) and texture (d), FLST - cartoon (e) and texture (f).	20
4-1	Dataset HDR images.	22
4-2	Belgium House. (a). Gradient Compression. (b). Bilateral filter. (c). Total variation.	24
4-3	Belgium House. (a). Nonlocal means (b). Cartoon+Texture (c). Cartoon+texture with the TV-L1. (d). Grain Filter.	26
4-4	National Cathedral, Washington, DC. (a). Gradient Compression. (b). Bilateral filter. (c). Total variation.	27
4-5	National Cathedral, Washington, DC. (a). Nonlocal means (b). Cartoon+Texture (c). Cartoon+texture with the TV-L1.	28
4-6	(a). Grain Filter for the Cathedral image. Goldstein Synagogue. (b). Gradient Compression. (c). Bilateral filter. (d). Total variation.	29
4-7	Goldstein Synagogue. (a). Nonlocal means (b). Cartoon+Texture (c). Cartoon+texture with the TV-L1. (d). Grain Filter.	30

1 Introduction

In the last years a boom in technology development of cameras and visual systems has occurred. Visual devices are able to recognize, process and enhance the information contained in the raw data in a very efficient way by incorporating in-built processors that take care of this treatment. This facility gives the opportunity to combine strong algorithms to tackle multiples limitations common in cameras, such as noise, blur, weak contrast, variable focus, limited resolution, etc [36].

Also, it makes it easier to extend the capabilities of the camera, in order to handle difficult scenes, particularly scenes under strong illumination or just the opposite, lacking of light. The problem behind the excess of light is that the sensor gets saturated which provokes an image with unnatural white regions. Whereas in the second case, the sensor is under exposed and unable to capture proficiently the information, because the signal is hidden by noise. In order to solve this problem, there exists approaches that are capable of enlarging the dynamic range of conventional cameras and that in some cases lead to recover the "true" radiance of any object in the scene. As a result of these approaches the obtained image is the so called HDR image, where HDR stands for High Dynamic Range. The idea lying behind this approach consists of merging intensity values that are acquired by the sensor under several exposition times such that the sensor will be able to capture properly regions under different illumination conditions. As a result of this process, the resulting information possesses a higher dynamic range than the images acquired under standard procedures which normally have integer intensity values ranging over 8 bits. Besides these efforts for recovering correctly the actual scene radiance by means of high dynamic approach, standard visualization and printing devices are not able to manage HDR data. Instead of building new devices, a convenient path is to modify HDR data for displays or conventional standard devices. Doing this requires rescaling properly the information in such a way that an ideal balance between the information offered by small and large intensities values occurs in order to obtain a visually appealing image that appears normal to the human visual system [28]. This task is usually referred to as HDR tone mapping.

Depending on the approach used, the tone mapping operation is susceptible to affect considerably the general aspect, quality or introduce artifacts in the image. In particular, the halo artifact is known to be one of the most annoying to photographers. It is characterized by an aura-like pattern at the borders of the objects, resulting in highly artificial appearance.

The aim of this thesis is to explore some classical approaches, as well as new alternatives,

to perform HDR tone mapping without introducing halo artifacts or affecting the details quality on the process. For that purpose we follow the scheme proposed in [18] where an image decomposition is carried out in order to obtain the information containing large scale variations (Base Layer) and another component holding small fluctuations (Detail Layer). Since the base layer possesses the larger range of variation, this is the component to be attenuated by certain factor. Then the detail layer I_D , which is eventually rescaled by factor k' , is added to the resulting image, as follows:

$$\begin{aligned} I_B &= \Phi_\lambda \{I_{HDR}\} \\ I_{TM} &= k \cdot I_B + k' \cdot \underbrace{(I_{HDR} - I_B)}_{I_D} \end{aligned} \tag{1-1}$$

Where Φ corresponds to the operator managing the extraction of the base layer I_B , a simplified image from the HDR data I_{HDR} . Parameter λ is a scale factor for the extraction and factor k compresses the base layer to a lower dynamic range. The above operations are carried out in the logarithm of the luminances, because it leads to a very simplified representation of the brightness and because pixel differences directly correspond to contrast in the log domain [42, 21].

The choice of the operator Φ will be driven by the fact that it should remove oscillatory behaviors while preserving edges. Therefore, when adding the detail layer back to the compressed base layer there will not be mismatches of regions that cause halo artifacts.

This document is organized as follows: A contextualization and review of popular methods are presented in Section 2. Section 3, presents the multiple alternatives proposed to deal with the tone mapping problem. In Section 4, a description of the experiments including the analysis of the results are given. Finally the concluding remarks are offered in Section 5.

2 Previous Work

HDR imaging is an important and appealing area in the field of photography mainly because it offers immunity to abrupt changes in illumination present in the scene. Along it, the possibility to observe details over the whole intensity range is an advantage that is exploited in several applications [37, 44, 6], such as film industry [38], computer graphics, image enhancement [26], medical imaging [10, 8, 9], etc. As mentioned in [38], HDR imaging is here to stay, offering a higher visual quality than traditional images. It is now used not only on technical areas but also in most consumer imaging devices, e.g. compact cameras and smartphones.



Figure 2-1: Conventional device enabled with HDR capabilities.

In the HDR imaging field there are two main tasks: creation and tone mapping. The first one involves obtaining the HDR radiance map. It usually (but not always) consists in merging different shots obtained with different acquisition times [38, 3]. The second one focuses on rendering high dynamic range scenes into lower dynamic range displays. Yet, there is also another alternative that aims to combine both creation and tone mapping notions to obtain in a single step a high quality representation of the scene. Those methods are called exposure fusion [29].

To better understand how HDR images are created [6], one important and early reference is the study carried out by [16]. In their study and taking as a departing point the fact that there is not a linear correspondence between digitalized intensity values with respect to the true radiance values in the scene, they report that nonlinear behavior is due to implicit

procedures carried out during the acquisition process within the so called camera response function. Knowing that the most extreme nonlinear behavior occurs in the saturation point, they propose a new alternative to cover the full dynamic range in troublesome scenes, such as the ones under sunlit conditions. Their solution consists in finding the characteristic curve of the camera using a set of images of the same scene captured under different exposure times; the nonlinear characteristic function serves to recover the radiance map of the scene which is supposed to hold the entire dynamic range in the images.

The characteristic curve is obtained in a least squared error manner assuming that the function to recover is monotonically increasing. The minimization problem which is a function of the irradiance values and exposure times of images also includes a second derivative of the estimate function in order to guarantee its smoothness. As a result of using the characteristic curve, they are able to recover high dynamic radiance maps from ordinary photographs. Since then, many methods have been proposed to perform HDR creation, see e.g. the state of the art in [3, 4]

Nevertheless, the dynamic range of current visualization devices is still limited and cannot manipulate HDR images. In order to convert a HDR image into an 8 bit image, there are mainly two alternatives, namely global mapping (also named tone reproductive curves) and spatially variant operators (also termed tone reproductive operators).

As part of global mapping methods, there are popular methods such as linear rescaling of the logarithm of the luminance, gamma correction and histogram equalization. Despite of being very practical and fast, they fail to conserve local contrast unaltered on regions where the image has a uniform behavior [21]. Other choices rely on models to correct the nonlinear mapping when digitalizing the scene [16] or propose methods that best resemble the adaptation behavior in the human visual system, such as physiology and perceptually inspired approaches [37, 28, 7, 25, 41, 22, 24].

Regarding the latter ones, some relevant contributions can be highlighted. In [41], being the first contribution of tone mapping in the area of computer graphics, they propose a psychophysical tone reproduction method for grayscale images taking inspiration from the human visual system (HVS) to solve the dynamic range compression problem. Their method tries to preserve brightness values that are modeled as a function of the adaptation luminance parameter and contrast sensitivity parameter. In the end, this operator converts the real world luminances to display values that best match the perceived brightness. In [24], the problem is managed in a multiscale approach based on the retinex theory. The retinex method is an algorithm that computes scenes reflectances based on color perception of the HVS. Their tone mapped image results from a linear combination of the retinex responses at different scales.

In [37] they focus on photoreceptors adaptation skills to implement a method that solves the tone mapping problem in HDR images. They rely on a perceptual model that is partially similar to the one of the human visual system. It basically consists of a global tone mapping

operator where the general idea of the model is to reproduce the ability photoreceptors possess to adjust automatically to different lighting conditions. In [28], they study contrast on images by following gradient domain and multiscale notions to incorporate visual perception on a tone mapping operation. They study the notion of contrast because it is a fundamental ability of human perception. As mentioned in their papers, the way we perceive the world is largely the result of our contrast adaptation machinery. Therefore, after introducing some contrast definitions that attempt to model the HVS contrast detection under specific stimulus, they introduce their own contrast model. Some parameters are introduced and studied like, contrast detection threshold and contrast discrimination threshold, which are the values at which the human visual system can distinguish contrast ('Contrast detection') in a uniform field and the value in which the human visual system HVS can spot the contrast difference between two identical stimulus.

Noticing that global tone mappings operators have difficulties to maintain contrast. In [22], Ferradans et al. propose a piecewise tone mapping curve followed by a local contrast enhancement algorithm. The tone mapping curve capitalizes the qualities of two popular perceptually based tone mapping operators: Naka-Rushton equation and Weber-Fechner's law. While the former measures our ability to spot tiny differences in intensity, the second one describes detectable difference thresholds for small stimulus. Since localized cone saturation is present in the human visual system, they integrate its contribution in the model. It is done by observing that the Weber-Fechner's law works well until just before the saturation point. Therefore, the authors replace that erroneous section by the corresponding section of the Naka-Rushton curve. As a second step process, the contrast enhancement method which is a perceptually inspired variational method is applied to the tone mapped image.

On the other hand, spatially variant operators allow to compute more accurate image representations by considering contextual information around each pixel. This capitalizes the assumption that the human vision is mainly sensitive to local contrast [34]. However the major drawback lies in the fact that these algorithms are computationally expensive and prone to include halo artifacts, [38, 31]. Halo artifacts can be more easily spotted as bright shadow patterns surrounding objects with dark intensity.

Within this approach, we highlight several relevant contributions, [21, 42, 18], which reduce significantly haloing artifacts. In [21], a method to compress the wide range on HDR images is proposed. Assuming that strong variations in HDR images lead to high gradient responses, they develop a method to compress the HDR gradient map, and after solving a Poisson equation they obtain the low dynamic range image. With the aim of having a gradual attenuation, gradient field reduction is performed in a multiscale way, so that high gradients will be reduced more than small gradients. This way, gradients associated with details shall be kept. Since performing integration is not guaranteed to exist when returning to the space of intensities, a Poisson equation is formulated by using the modified gradient field. In their implementation they use a finite difference scheme that is solved through a multigrid algorithm.

Inspired by the way artists include detail gradually on their paintings, [42] proposes a hierarchical scheme to reduce contrast on HDR images. Their method is motivated by anisotropic diffusion method. They decompose the image in a multiscale manner so that they are able to maintain detail at every scale. In the end the weighted detail components are added back to the compressed coarser image. The way they obtain an image having both intra-object smooth and inter-object sharp qualities, is by defining a set of PDE's that intend to set curvature to zero or infinite.

Similarly, in [18] a technique for displaying HDR images is proposed based on the fact that an image can be represented as the sum of its frequency components, namely low frequencies corresponding to smooth regions and high frequencies associated to edges and detail. In their study, they propose to use a fast version of the bilateral filter to extract a base component from the HDR image. The base layer is compressed a certain factor and subsequently the detail layer is added to it, hence reducing the dynamic range of the image while preserving details. The bilateral filter is computed as a constrained average of intensities where the criterion to sum is driven by an influence function that evaluates if the differences between the actual pixel and its surroundings are small. Therefore, this concept resembles anisotropic diffusion. This way, when there is a large difference of intensities, like at borders, the intensities will be penalized with a small weight. In the end, a smooth image that preserves edges will be obtained. Their contribution lies in two aspects. The first one, is related to robust statistics, helps them to compute a fast bilateral filtering by using *FFT*. The second one is related to the method to reduce the dynamic range on HDR images.

We found that most of the methods dealing with HDR reduction perform their tasks in the luminance channel, which is subsequently used to compute the RGB image in order to maintain a uniform correspondence between colors [28].

Although visual perception is very subjective and every algorithm will likely have different impact on the viewer, the general pros and cons of tone mapping approaches can be stated as follows: global tone mapping methods fail to maintain detail when compressing the range of the image but it does conserve brightness, overall contrast and color [13]. Because of its simplicity and fast speeds it can be a suitable option to generate images for low level applications where detail is not a main concern. With regard to local tone mapping, it is more computationally demanding, sometimes difficult to tune for particular images and is prone to halo artifacts. However, if properly set, it succeeds in capturing the essence of the scene giving a more vivid and natural aspect.

In this study, we chose to work with the spatially variant approach. We will follow the idea of decomposing the image in two components referring to one holding large scale variations (Base layer) and another one keeping texture and details. For that reason, several popular edge-preserving filters were studied. Such filters include anisotropic diffusion [35], total

variation [39], nonlocal denoising [11], cartoon/texture image decomposition [12, 23] and area-filter driven by the fast level set transform [32].

A pioneering study about edge preserving methods is [35]. Starting with an analysis about multiscale Gaussian decomposition, they indicate that this description process resembles the heat conduction equation and that it is an inappropriate model to maintain edges. It is basically because of the Gaussian filter that blurs the edges of the objects. In order to allow the diffusion exclusively in uniform regions and not at edges, they propose to solve an anisotropic diffusion equation. In the model they include a term that regulates the diffusion. That term is referred to as the stopping function that stops the diffusion process on edges. It is basically a monotonically decreasing function that is one when values are close to zero and vanishes when the input acquires larger values. As an initial estimator of edges they use the gradient operator for the simplicity it offers. They also show that edge enhancement can be achieved depending on the stopping function.

A related approach is [39] where a method to remove noise on images is proposed. It is based on a constrained minimization problem involving the total variation of the image. Although it was firstly avoided because it leads to nonlinearities, several studies showed that L_1 norm is appropriate for image restoration purposes giving the advantage of removing noise while conserving sharps edges. A smooth image can be obtained by using gradient descent method, or more efficiently using projection methods [14], and it is expected to reach its steady version when the parameter t tends to infinity.

In [11], a filter relying on adaptive averaging is proposed. Pixel values are averaged on elements with similar intensities or similar local neighborhoods. Since these values are not necessarily local, this is known as non-local means denoising. For asserting the similarity between the neighborhood associated to certain pixels, they use a weighted L_2 norm. In this sense the final quality of the resulting image is depending mostly on how repetitive is the region that is surrounding each pixel.

Aiming for an edge preserving smoothing method, the study in [12] can be seen as a linear combination of the original image and the low pass filtered image. The weights governing the linear combination are set according to how variable is the behavior in the current position. In this sense, the method will assign more priority to the original intensity if the location does not present an oscillatory behavior. Conversely, there will be more proportion of the smoothed image if the original image presents oscillatory components on that region. More importantly is the way to identify the amount of oscillations on the image, for that purpose they rely on the proportion of change of the total variation of the image when compared to the total variation of a low pass filtered version of the original image. An appropriate tuning of the weighting function enables the method to remove fine details from the image and maintain step edges on the cartoon side.

The last method we include in our experiments is the work developed by Pascal Monasse [32]

in which an image representation insensitive to contrast changes is developed. This image representation consists in a tree of shapes that is generated by combining the upper and inferior set of level sets of the image, where each node is nothing but the geometric closed shape of that level. The criterion to add children to each node depends on whether the children is contained within that current shape or not. If not, another father will be created. Analogously, each branch in the tree can be interpreted as an object; set of shapes defining an element in the image, which is lying just in other element. Whereas leafs can be seen as small oscillations lying over smooth image structures. Upon smoothness of that object, each branch will contain a shape that is gradually getting smaller. In order to extend the applications of the method, the author also proposed a grain filter which eliminates small shapes of the tree which results in a denoising method.

With the intention to capitalize the later approach, in this study we use [32] as a good alternative to decompose the original image in base and detail components, inspired in the fact that after removing small shapes, this representation does not modify original characteristics of the image, especially in the borders.

3 Algorithms Studied

From the previous section we know that despite the large variety of methods for attacking the tone mapping problem, there are still some gaps and challenges that have not been solved yet for both approaches, local and global operators. For example, the trade-off between parameter calibration and color consistency in the resulting image is a trial and error task. Also, trying to model accurately the human perception is not an easy task and the model should use simple approximations to reduce computational costs, also it might suffer of an excessive amount of parameters driving the model.

Based on that, during the course of this stage several algorithms were studied and implemented in order to be familiar with the problem and identify the usual problems at which current methods are prone to. Additionally, it allows establishing a comparative analysis to identify which one behaves better for our purpose. Therefore they will be described in the remaining of this section.

Particularly, the tone mapping operators used in this study rely on gradient map modifications and image decomposition to reduce halo artifacts in the resulting image. Since the latter approach offers a direct route to range compression we also explore multiple alternatives in the same spirit.

3.1 HDR Compression Methods: Two Classical Methods

This section is dedicated to present two important methods from the literature. Given their wide acceptance for being efficient at tone mapping without introducing halo artifacts, they have been implemented and taken as reference point for later analysis.

3.1.1 Gradient Based Approach

The first method studied is the gradient high dynamic range compression developed by Fattal et al. [21]. They were inspired by the premise that drastic changes in the luminance channel lead to large gradient responses, whereas detail and texture elements possess gradients of smaller magnitudes. The attenuation of large magnitude gradients is handled in a multiscale fashion by finding the corresponding weights that will be applied locally on the gradient map. A compressed HDR image will be reconstructed based on the new gradient map.

Let $L(x, y)$ be the logarithm of the luminance channel associated to the HDR image. The compressed gradient map is nothing but the product of the image gradient $\nabla L(x, y)$ and a

weight function Φ , as follows:

$$C(x, y) = \nabla L(x, y) \cdot \Phi(x, y) \quad (3-1)$$

In the above equation, the weight function have to be computed such that no contrast inversion should occur, otherwise the appearance of the final image would be impaired. For that reason, only gradient magnitudes will be processed.

For computing the weight function, a multiscale approach is performed in order to capture the contribution of gradients at different scales. The integration of all weights computed at each scale is done through an iterative multiplication, hence the attenuation value will be propagated from one scale to the other.

The proposed expression to compute the weight function at scale k is a function of the magnitude of the gradient calculated for each scale in the Gaussian pyramid of image $L(x, y)$, as showed below:

$$\phi_k(x, y) = \frac{\alpha}{\|\nabla L_k(x, y)\|} \left(\frac{\|\nabla L_k(x, y)\|}{\alpha} \right)^\beta \quad (3-2)$$

Where k gets values from 0 to d , $L_{k=0}$ is the original image and will be iteratively smoothed and reduced until it is at least 32 on its width and height.

Function ϕ_k is tuned by using parameters α and β . Parameter α establishes the limit where gradient values should be enlarged or reduced. For that reason, it is proposed to be set as a tenth of the average value in the current gradient field. Parameter β regulates how strong the attenuation or amplification is; in [21], it is recommended to set it between [0.8 0.9].

Equation (3-2), the gradient at scale k is computed using central differences.

$$\nabla L_k = \left(\frac{L_k(x+1, y) - L_k(x-1, y)}{2^{k+1}}, \frac{L_k(x, y+1) - L_k(x, y-1)}{2^{k+1}} \right) \quad (3-3)$$

Now that the weight function has been computed, the next step is to return from the gradient map to the space of intensities. Since we have no guarantee that the field $C(x, y)$ resulting from equation (3-1) is conservative there might not be an image I accomplishing $C = \nabla I$. Then, an additional analysis is performed. It is proposed to find the image I in the space of 2D functions, such that its gradient minimizes the least square error, as in the following expression:

$$\text{minimize } \iint \|\nabla I - C\|^2 \partial x \partial y \quad (3-4)$$

Where

$$F = \|\nabla I - C\|^2 = \left(\frac{\partial I}{\partial x} - C_x \right)^2 + \left(\frac{\partial I}{\partial y} - C_y \right)^2 \quad (3-5)$$

According to the variational principle, the image I should satisfy also the Euler-Lagrange equation, as presented in [21].

$$\frac{\partial F}{\partial I} - \frac{\partial}{\partial x} \frac{\partial F}{\partial I_x} - \frac{\partial}{\partial y} \frac{\partial F}{\partial I_y} = 0 \quad (3-6)$$

Solving Equations (3-5), (3-6) and rearranging, we obtain the Poisson equation:

$$\nabla^2 I = \text{div } C \quad (3-7)$$

Which is a linear differential equation that is solved as proposed in [17]. Their approach relies on the FFT which is applied to the matrix representation of the Poisson equation. By using finite differences on the Laplacian of image I , the matrix representation is:

$$T * I + I * T = \underbrace{\text{div } C}_B \quad (3-8)$$

Where

$$T = \begin{bmatrix} 2 & -1 & 0 & \cdots & 0 \\ -1 & 2 & -1 & \vdots & \vdots \\ 0 & -1 & \ddots & -1 & 0 \\ \vdots & \vdots & -1 & 2 & -1 \\ 0 & \cdots & 0 & -1 & 2 \end{bmatrix} \quad (3-9)$$

After applying singular value decomposition $T = Q * \lambda * \text{inv}(Q)$ to solve for I , the high-level algorithm is stated below:

1. Compute $\bar{B} = \text{inv}(Q) * B * Q$
2. For each element in i, j in the matrix, compute: $\bar{I}(i, j) = \frac{\bar{B}(i, j)}{(\lambda(i, i) + \lambda(j, j))}$
3. Compute $I = Q * \bar{I} * \text{inv}(Q)$

Where the eigenvalues λ and eigenvectors Q for matrix $T_{n \times n}$ can be calculated as:

$$\lambda(j, j) = 2 * \left(1 - \cos \left(\frac{j * \pi}{n + 1} \right) \right) \quad (3-10)$$

And

$$Q(i, j) = \sin \left(\frac{i * j * \pi}{n + 1} \right) * \sqrt{\frac{2}{n + 1}} \quad (3-11)$$

3.1.2 Base and detail image decomposition by using the bilateral filter

Being one of the best methods in tone mapping [31], the present operator proposed by Durand and Dorsey in [18], relies on image decomposition to compress the dynamic range of the HDR image. It basically attenuates a smoothed version of the original data to which the detail component is reintegrated.

For the purpose of image decomposition, namely base and detail, they study the bilateral filtering, which is a kind of filter that preserves edges while smoothing surfaces.

Inspired in anisotropic diffusion, bilateral filtering is a nonlinear filter developed by Tomasi [40]. This filter consider both spatial and intensity information to compute a weighted average of the input. The function managing the spatial information is the traditional Gaussian filter f , whereas the function that handles intensity information is a redescending curve g that decreases the weight of pixels with large intensity differences. In that sense function g , resembles the edge-stopping function in anisotropic diffusion. The output of bilateral filtering is expressed as below:

$$J_s = \frac{1}{k(s)} \sum_{p \in \Omega} f(p - s) \cdot g(I_p - I_s) I_p \quad (3-12)$$

Where s is the coordinate of each pixel in the domain Ω of image I , and the normalization factor $k(s)$ is computed as:

$$k(s) = \sum_{p \in \Omega} f(p - s) \cdot g(I_p - I_s) \quad (3-13)$$

It is expected from equation 3-12 that differences of intensities lying in the same neighborhood will be affected inversely to its amount of change. In the case I_s belongs to a border, this is equivalent to say that function f will be attenuated less by function g , which leads to a weaker smoothing than for "regular" surfaces.

Knowing that function g should be large for small domain values and reduce progressively on large domain values, the proposed influence function used in the original bilateral filtering is a Gaussian function. However other curves are also studied in [18], such as the Lorentz, Huber and Tukey's biweight function. However, after noticing not significant difference while compared to Tukey's function, they use the Gaussian curve as the influence function in their implementation.

In our implementation, in order to avoid long computational times we make use of Matlab's capabilities to handle matrixes, for that purpose we use a matrix formulation of the problem instead of point to point expressions. As in [18], we also use the Gaussian kernel to smooth the image and the Gaussian function as the influence function. Moreover, instead of computing over the whole image domain, we use a patch of particular size around the current pixel I_s . A suitable patch has a size of 11x11 pxls.

As mentioned earlier, the dynamic range compression is managed on the base layer resulting from the bilateral filtering that was tuned under specific parameters σ and size of the spatial kernel. They propose to compute an intensity image as input for the bilateral filtering. Since it gives a more uniform treatment for the whole image range, the intensity image is transformed to the log domain to perform the subsequent processing stages. To maintain color correspondence, each color channel is split by the input intensity and then multiplied by its processed version to recompose the compressed HDR image.

Although the attenuation is specified by the user, in the original paper the authors suggest to use a compression factor of $k = 5$ log units in their implementation. However, it should be modified when the image contains light sources.

The high-level algorithm for dynamic range compression proposed by the authors (visit also [19]) is shown below:

1. Compute input intensity. $I_{in} = \frac{1}{61 \cdot (20 \cdot R + 40 \cdot G + B)}$
2. Extract input intensity from each channel. $r = \frac{R}{I_{in}}, g = \frac{G}{I_{in}}, b = \frac{B}{I_{in}}$
3. $L_{Base} = \text{Bilateral Filtering}(\log(I_{in}))$
4. $L_{Detail} = \log(I_{in}) - L_{Base}$
5. $L_{out} = L_{Base} \cdot k + L_{Detail} - As$
6. Construct the output image.

$$\begin{aligned}
 R_{out} &= r \cdot \exp(L_{out}) \\
 G_{out} &= g \cdot \exp(L_{out}) \\
 B_{out} &= b \cdot \exp(L_{out})
 \end{aligned} \tag{3-14}$$

Where As is a normalization factor that moves the data up to one. It is computed as $As = \max(L_{Base}) \cdot k$.

After computing the new color channels, a new normalization is applied to obtain a dynamic range of 8 bits. But, since few pixels in the resulting image go beyond the largest allowed value, the normalization should be done without including those values. Otherwise, the largest values would attenuate the impact of small intensities. A simple way to avoid this is by clipping those intensities and assigning them to 255. Another alternative is to saturate a fixed percentage of the values, approach used in [28] after recovering the tone mapped image.

3.2 Using Denoising and Geometry/Texture filters for image decomposition

As seen in the previous section, the Fast Bilateral Filter for high dynamic reduction gives a rather direct path to obtain a tone mapped image by simply using a small set of parameters that can be user-controlled. That tradeoff between simplicity and efficiency offered by Durand and Dorsey's method [18] encourage us to explore it further in the area of image decomposition. In this sense, we explore some alternatives of decomposition methods that could work better to extract the base layer than the bilateral filter. Like the bilateral filter they should remove small scale components without modifying edges associated to large scale objects. In other words, they should get rid of high frequency components without blurring edges. Based on that, methods fitting those requirements are denoising operators or more adequately cartoon-texture decomposition methods.

Before stating how to use edge preserving algorithms for tone mapping, in the remaining of this section we present some methods of this class for later purposes of evaluation and particularly to answer how efficient they are to handle halo artifacts and quality of the image.

3.2.1 Total variation

This algorithm, introduced by Rudin et al. [39] intends to remove noise in images by using a nonlinear total variation scheme. The general idea is to obtain a smoothed version u of the noisy image v by solving a minimization problem expressed as a regularization part relying on total variation and a fidelity term.

From an observation $v(x, y)$ equal to a clean image corrupted by additive noise $n(x, y)$, one wishes to recover the image u ,

$$v(x, y) = u(x, y) + n(x, y) \quad (3-15)$$

The formulation of the problem is the following:

$$\arg \min_u \iint_{\Omega} \|\nabla u(x, y)\|_2 \partial x \partial y + \lambda \iint_{\Omega} |v(x, y) - u(x, y)|^2 \partial x \partial y \quad (3-16)$$

Where λ is a given scale factor that controls the degree of smoothing in the process.

In the original paper, the optimization problem shown in Equation (3-16) is solved by using the gradient descent method. A denoised version of the image is obtained for a large number of iterations. More recently, a projection method was introduced in [14] to solve the total variation problem more efficiently.

3.2.2 Non local means

The nonlocal means method for image denoising was proposed by Buades et al. [11]. It has been a true breakthrough in the field of denoising and has since triggered a large number of works. The method is mainly derived from the observation that classical denoising methods rely on the average of pixel intensity. However, it is also mentioned that averaging intensities corrupts the output image by blurring borders, which goes against the general purpose of denoising where noise should be removed without altering the quality of the original image. As an alternative, it is proposed in [11] to denoise images by averaging the values of pixels having a similar neighborhood.

As in the previous case, the goal of nonlocal means method is to recover the denoised version u from a noisy image $v = \{v(i) | i \in I\}$, as in Equation (3-15).

The nonlocal mean algorithm is defined by the expression:

$$NL[v](i) = \sum_{j \in I} w(i, j) v(j) \quad (3-17)$$

The family of weights $\{w(i, j)\}_j$ is given by:

$$w(i, j) = \frac{1}{Z(i)} e^{-\frac{\|v(N_i) - v(N_j)\|_2^2}{h^2}} \quad (3-18)$$

Where N_k denotes a square neighborhood of pixel k and $Z(i)$ is a normalizing constant given by.

$$Z(i) = \sum_j e^{-\frac{\|v(N_i) - v(N_j)\|_2^2}{h^2}} \quad (3-19)$$

The parameter h controls the decay of the Gaussian function, and therefore the tolerance given when averaging similar pixels.

Equation (3-17) is an averaging of pairs of similar intensities and establishes an impact proportional to their difference. The impact is governed by the Gaussian function which will be large when the neighborhood of pixels are comparable and small otherwise. Also, it means that the image will be smoothed stronger only if the current neighborhood possesses similar neighborhoods to the ones it is being compared with.

A priori, a good denoising method is not efficient to separate the image into base and details as it is looked for in HDR tone mapping. In this sense the method proposed in [18] actually relies on the limitations of the bilateral filter. However, we will include the nonlocal means in our study in order to have a comparison point with [18].

3.2.3 Cartoon+Texture

Many variational methods have been introduced to decompose an image into geometric and texture components, following the seminal work by Y. Meyer [30] and the first implementations by [43] and [5]. In this work, we focus on a simple and efficient approach proposed in [12]. The method deals with the image decomposition in a frequency-like approach. The idea is to extract the cartoon component, which contains mostly small frequencies but also large frequency associated to borders, from the original image. Once the cartoon component is found the extraction of the detail component is straightforward, as the difference between the original image and the cartoon component. Conversely, the texture component is endowed mostly with high frequencies and partial contribution of middle frequencies.

As several previous contributions on the topic, the problem is approached as a variational problem by assuming that the cartoon part has a minimal total variation. This time, the authors of [12] integrate the local influence of the texture part while assuming that it possesses a fast decay in the total variation after the neighborhood has been smoothed. In this sense, they compute the proportion of change of the smoothed local variation respect to the original local variation, which is named relative reduction rate.

In the end, a weighted sum is proposed between the original image and its smoothed version. The weights will be large for high relative reduction rates, meaning intensities lying in textures, and small if the intensities belong to border regions, or equally small relative reduction rate. In other words, the lower the relative reduction rate, the higher the contribution of the original intensities in the output.

Given the input noisy image $u(x)$, the smoothed local total variation at pixel x is:

$$LTV_\sigma(x)(u) = G_\sigma * |\nabla u|(x) \quad (3-20)$$

Where G_σ is a Gaussian kernel with standard deviation σ .

The relative reduction rate of the local total variation is computed as follows:

$$\lambda(x) = \frac{LTV_\sigma(x)(u) - LTV_\sigma(L_\sigma * u)}{LTV_\sigma(x)(u)} \quad (3-21)$$

Where L_σ is a low pass filter.

The output of the method for the cartoon component is presented below:

$$kr(x) = w(\lambda(x)) \cdot L_\sigma * u + (1 - w(\lambda(x))) \cdot u \quad (3-22)$$

Where $w(x) : [0 \ 1] \rightarrow [0 \ 1]$ is a piecewise crescent function as shown in figure 3-1.

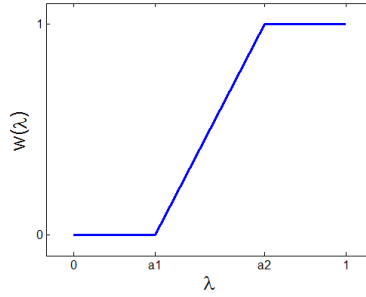


Figure 3-1: Influence function.

3.2.4 Cartoon+Texture with the TV-L1

An alternative model for geometry/texture separation is the TV-L1 model [33].

The total variation with L1 norm (TV-L1) is:

$$\min_u \lambda \|u - g\|_1 + \|\nabla u\|_1 \quad (3-23)$$

Where g is the original image and the resulting cartoon component will be obtained in u^* .

The discrete L1 norm is defined by $\|u\|_1 = \sum_{i,j} |u_{ij}|$.

It is known [20] to extract details from the image depending on the ratio perimeter/area. Therefore small and elongated shapes are put in the texture part untouched. Consequently, it seems an interesting candidate for tone mapping. In order to solve the variational problem, in this work we chose to use the implementation developed by Le Guen [23]. He relies on the method developed by Chambolle and Pock [15] in which a first order primal dual algorithm is proposed.

Through experiments it is established that, the smaller the scale factor λ is, a more cartoonized image is obtained.

3.2.5 Fast level set transform

Within the class of connected filters, the grain filter derived from the fast level set transform (FLST) proposed by Monasse in [32] offers a framework that is interesting to study in the tone mapping setting. Due to its efficiency and configuration, we think that the FLST has a meaningful potential to separate properly the image in a cartoon and detail components, therefore leading to a proper performance when reducing the dynamic range of the image. The idea behind the fast level set transform is to find an image representation that is invariant to local contrast changes. This makes it suitable for applications where illumination

changes constantly. In order to compute the image representation, Monasse approaches the problem in a level set scheme. It is by extracting the connected components that are lately rearranged, as shapes, in a tree. Specifically, a shape is a connected component of a level set that has its holes filled.

The upper level set X^λ of λ and lower level set X^μ of μ extracted from image u are defined as:

$$\begin{aligned} X^\lambda &= \{x \mid u(x) \geq \lambda\} \\ X_\mu &= \{x \mid u(x) \leq \mu\} \end{aligned} \tag{3-24}$$

It is known that the data contained in each of the level set previously shows is enough to reconstruct image u .

$$u(x) = \sup \{\lambda \mid x \in X^\lambda\} = \inf \{\mu \mid x \in X_\mu\} \tag{3-25}$$

The inclusion structure of both these sets is used to construct a tree made of all shapes. For the detailed set of steps necessary to compute the fast level set, see [32].

After computing the tree of shapes, the grain filter is computed directly by removing the shapes whose area is not larger than certain threshold Th .

3.2.6 Examples

This section is dedicated to illustrate the performance of the methods presented before as potential alternatives for image decomposition, namely, total variation, nonlocal means, cartoon + texture, cartoon + texture TV-L1 and grain filter. For that reason an image including a large display of textures and regular regions is selected, see figure 3-2(a). In the set of images located below, the output of the methods, called base layer for our purpose, is presented beside the texture component. As mentioned earlier, the texture component is simply the base layer subtracted from the original image.

Figures 3-2(b) and 3-2(c) show the outcome pair base-detail for the total variation approach with scale factor equal to $\lambda = 40$. The nonlocal means method was tuned with $\sigma = 40$, figure 3-2(d). Figure 3-3(a), shows the output for cartoon+texture [12] tuned with scale factor $\lambda = 2$. For cartoon + texture using TV-L1 the scale factor is $\lambda = 1.3$, see figure 3-3(c). Finally, the grain filter via FLST is obtained by discarding shapes smaller than 100 pxls, see figure 3-3(e).



(a)



(b)



(c)



(d)



(e)

Figure 3-2: (a). House in the field image. Output of the filters for: Total variation - cartoon (b) and texture (c), Nonlocal Means - cartoon (d) and texture (e).

Although parameter calibration plays a very important role in the aspect of the resulting image, from the images presented above, it is visible that the methods achieving more cartoon like aspect are the grain filter, cartoon+texture TV-L1 and Total variation. This is because they lead to piecewise regular surfaces in regions where there is a concentration of details, just like in the trees where leafs have been merged in one single region depending on their intensity. Regarding the other methods, nonlocal means presents a smooth transition in

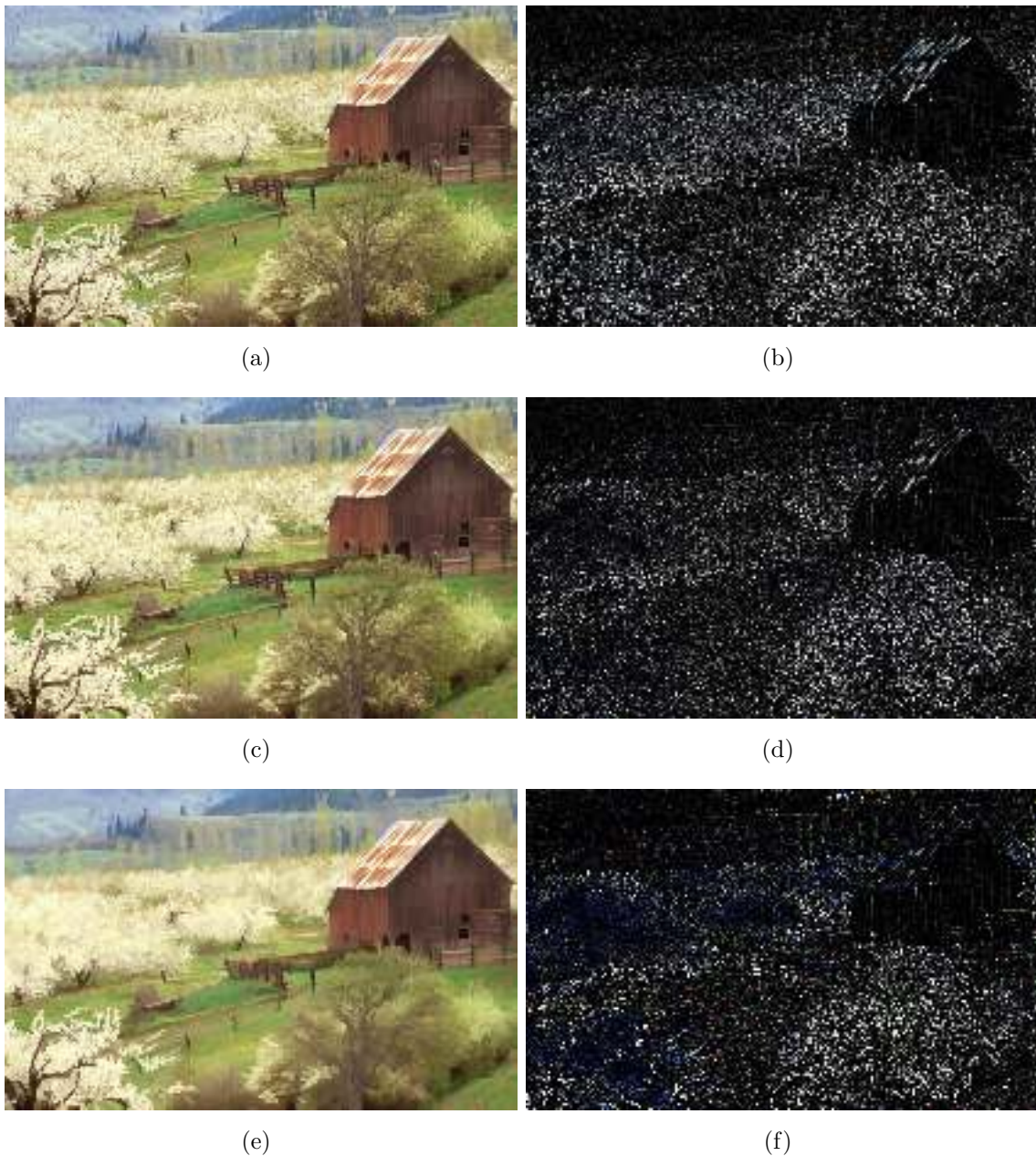


Figure 3-3: Output of the filters for: cartoon + texture - cartoon (a) and texture (b). cartoon - texture L1 - cartoon (c) and texture (d), FLST - cartoon (e) and texture (f).

objects that are not highly contrasted as in the paths leading to the house, where they seem to disappear mixing with the surrounding grass. For this image, cartoon+texture gives a smooth aspect on highly textured regions.

4 Experiments and Results

In the previous chapter, two classical methods for reducing the dynamic range of HDR images were described, gradient domain compression and fast bilateral filter for tone mapping. Also, several methods dealing with image decomposition were presented in order to be used in the general framework of [18] for tone mapping purposes.

In this section, several experiments are performed with the aim of evaluating the methods for high dynamic range reduction. In the evaluation we focus our attention on the quality of the resulting image, halo impact and difficulty on parameter calibration. For that purpose, the aforementioned tone mapping classical methods were implemented (in Matlab) as a reference point. Regarding the remaining algorithms, we made use of two scientific tools containing the implementation of the methods, namely MegaWave and IPOL which are publicly available at [1] and [2], respectively.

4.1 Implementation for the HDR tone mapping methods

4.1.1 Gradient domain compression

Computing this method involves four main stages, weight function generation via multiscale decomposition, gradient map compression, solving the Poisson equation and image recomposition. As mentioned in the original paper, the weight function can be computed by extracting the gradient in each tile of the Gaussian pyramid. For that reason, we considered that $\sigma = 5$ was appropriate for smoothing the image. For resizing the images we used cubic interpolation. As suggested by the authors, we set $\alpha = 0.1$ and $\beta = 0.8$.

The gradient map compression is computed through a pointwise multiplication between the found weight function and the original gradient map extracted by forward differences. Solving the Poisson equation on the modified gradient map was carried out by using matrix decomposition as shown in Section 3.1.1 which leads to a direct factorization of the resulting image. All computations were performed in the log domain of the HDR image. As showed in the paper, reconstructing the color image is performed by relying on the rate of change between the initial RGB channel and the output of the method. The operation is powered by a factor s managing the saturation of the colors. Explicitly the RGB tone mapped image is computed as follows:

$$C_{out} = \left(\frac{C_{in}}{L_{in}} \right)^s L_{out} \quad (4-1)$$

Where $C_{in} = R, G, B$. Parameters L_{in} and L_{out} correspond to the original luminance channel and processed luminance channel after being applied the inverse of the logarithm.

4.1.2 Bilateral Filter for tone mapping

For tone mapping purposes, implementing this method implies extracting the base layer via bilateral filter, computing the detail layer, adding the detail layer back to the compressed base layer and reconstructing the RGB tone mapped image.

Bilateral filter is a method that applies a spatial filter followed by an intensity influence function over the whole image. In order to speed up the method, the spatial filter is approached in neighboring patches of certain size. For that purpose we made use of Matlab's capabilities to deal with matrices. The original luminance channel of the HDR image is decomposed in small patches centered at each pixel, then applying the Gaussian kernel and the influence function is direct. Since there is a resulting pixel for each processed patch, the output image is reconstructed from this set of values. The bilateral filter should be tuned by three parameters, namely, size of the patch, sigma for the Gaussian kernel and sigma for the influence function. The rest of the implementation is direct and it can be easily done by proceeding like in the algorithm shown in Section 3.1.2.

4.2 Dataset and evaluation protocol

For evaluating the methods we worked with a set of popular images widely used in the HDR community, figure 4-1. The dataset contains HDR images that can be downloaded from the web, courtesy of Lischinski [27]. Being mostly natural and indoors scenes, the images are themselves a challenge for tone mapping algorithms because they are endowed with an important display of textures, regular zones and highly contrasted regions.



Figure 4-1: Dataset HDR images.

Since there is not a standardized automatic method to evaluate tone mapping algorithms, in this study we assess the methods in a qualitative manner by analyzing the effect of the

parameter tuning and comparing the results in terms of visual quality, halo’s artifact and difficulty on parameter tweaking to reach a visually appealing image.

4.3 Experimental Settings

As mentioned earlier, the purpose of this study is to analyze several geometric methods in the general framework of fast bilateral filtering for tone mapping [18]. Following Durand et al., the aim is to get a base layer that will be compressed. In this case, the base layer will be computed by using the denoising and geometric filters detailed before, the resulting image can be easily introduced in the implementation of [18] by replacing the line 3 in the algorithm presented in section 3.1.2. A particular set of parameters were used and an analysis is provided based on the results. For the parameters utilized for each method, please refer to table 4-1.

Methods	Parameters
Gradient Compression [21]	$\sigma_{kr} = 5$ $s = 0.6$
Bilateral Filter [18]	Kernel size = 11, $\sigma_{kr} = 5$ $\sigma_{int} = 1$
Total Variation	Scale factor = 2, 5, 10, 15, 20, 25.
Nonlocal Means	Scale factor = 20
Cartoon/Texture	Scale factor = 5, 8, 10, 15.
Cartoon/Texture TVL1	Scale factor = 0.2, 0.5, 1, 2.
Grain Filter	Removal threshold = 500

Table 4-1: Parameters of the methods for the experiments.

4.4 Results

For practical visualization, the outputs are displayed in a set of three images per experiment, where they are organized in the next sequence: base, detail and tone mapped image. Although several parameters were included, only the images with the most convenient parameter are presented, they are highlighted in color red within the table. For the Belgium House see figures 4-2 and 4-3. For the National Cathedral see figures 4-4 and 4-5. For Goldstein Synagogue refer to figures 4-6 and 4-7.

4.5 Analysis

After carrying out a close observation of each output, the gradient compression method, bilateral filter, nonlocal means and grain filter, work good with a default parameter for almost all images, hence being more robust to parameter tuning. Whereas for the remaining



(a)



(b)



(c)

Figure 4-2: Belgium House. (a). Gradient Compression. (b). Bilateral filter. (c). Total variation.

methods, the trial and error was more tedious, requiring several changes on parameters until a more stable output was obtained.

Particularly, the scale factor for the total variation method improves the tone mapping operation when growing up to 25. Otherwise a smoother image is obtained in the base extraction, leading to halo artifacts. For cartoon/texture it was the opposite, the larger the scale factor, the smoother the base layer. A suitable balance between smoothness on regular regions and

sharpness at edges was found with the scale factor equal to 8. The case for cartoon/texture TV-L1 was more complicated showing strong dependency to the parameter choice, therefore the election of the steady value was more difficult. Specifically, a predominant cartoon image would be obtained with scale values close to zero. In this case, an appropriate output was obtained when the scale factor was 0.5.

In these experiments, the images had an average size of 1000x770 pxls and the processing time rounded 15 secs for all the methods, except for cartoon+texture and nonlocal means which required approximately one minute to process the image.

Regarding the visual aspect, all the images presented a subtle absence of illumination. This is because, the compression factor is image dependent and trying to find a value that leads to fit appropriately the original high dynamic range into an 8bit range is not simple task. First, a problematic situation arises when relocating the luminance processed channel in the log domain is not well performed. Secondly, the detail layer can also modify easily the resulting image if its components are larger than the base layer after compression. Another side effect is presented when texture is altered considerably which could facilitate the excess of details in the resulting images, as in bilateral filter, gradient domain compression, cartoon/texture and nonlocal means, or just the opposite by removing the texture leading to flat zones in the resulting image as in total variation for small factor scale values.

With respect to halo artifacts, the worst case scenario was obtained with cartoon/texture where edges were blurred strongly leading to a large mismatching of values between the base layer and the detail layer. Alternatively, it means that cartoon+texture gave more priority to the smooth component than the original component in the linear combination. Also as it was probable, nonlocal means had a bad performance. Since it was developed to extract noise, an amplification of noise was implicitly taking place in the tone mapping task. Nevertheless, the fact that halo artifact appeared in the resulting image was because edges were also quite blurred.

In our opinion the best methods for tone mapping that did not include halo artifacts were cartoon+texture TV-L1 and the grain filter. And it was because they removed mostly all texture components without affecting the quality at edges. This result shows the capabilities of both methods to decompose images in cartoon and texture components as mentioned in [23, 20]. However, each one of those two, have certain disadvantages that can corrupt slightly the output. For TV-L1, it was clearly stated in [20] that this method removes from the image elements having a ratio perimeter/area lower than a factor, such as straight lines. In this case, the detail image resulting from the TV-L1 possesses several elements that were classified as texture, for example the top gap between the frame of the door appears well defined, this leads to a saturation in the resulting image. In the other case, the base layer can be corrupted when the grain filter assigns a strong contrast to the removed shapes leading to non-natural appearances.



(a)



(b)



(c)

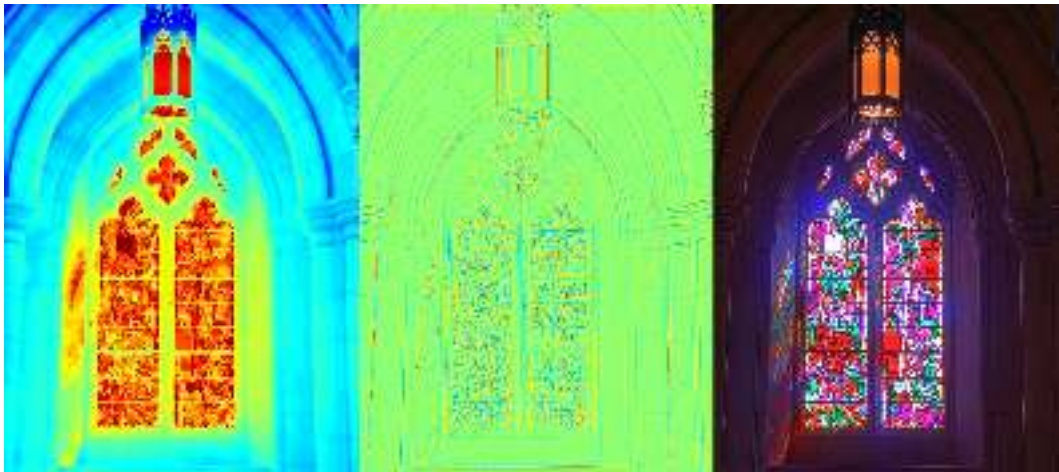


(d)

Figure 4-3: Belgium House. (a). Nonlocal means (b). Cartoon+Texture (c). Cartoon+texture with the TV-L1. (d). Grain Filter.



(a)

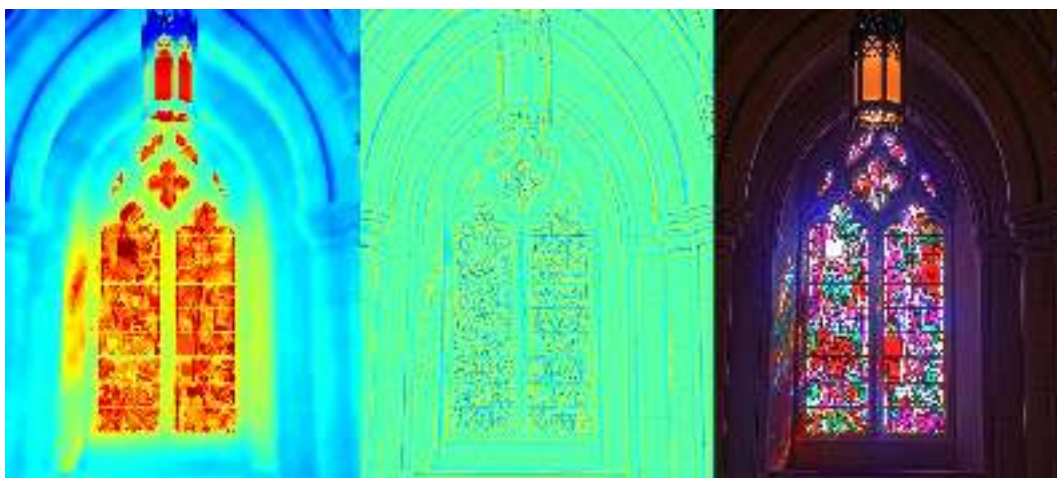


(b)



(c)

Figure 4-4: National Cathedral, Washington, DC. (a). Gradient Compression. (b). Bilateral filter. (c). Total variation.



(a)

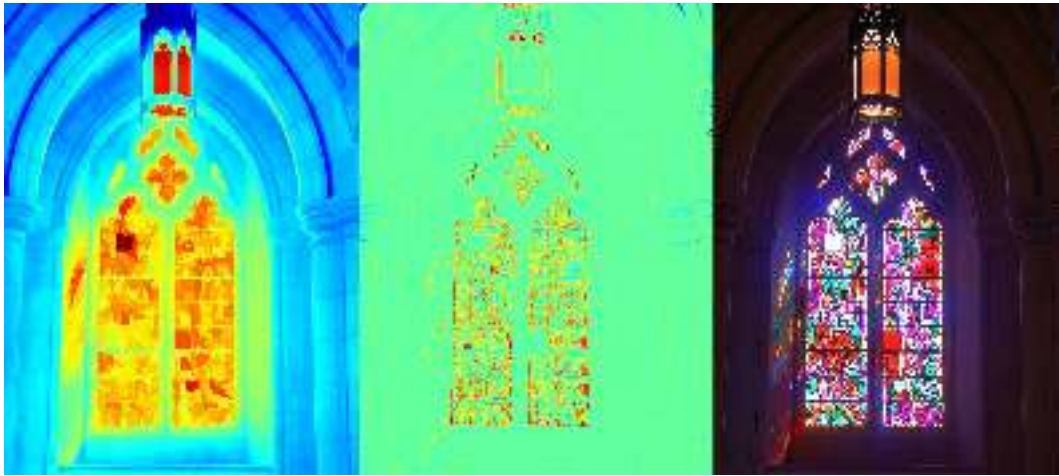


(b)



(c)

Figure 4-5: National Cathedral, Washington, DC. (a). Nonlocal means (b). Cartoon+Texture (c). Cartoon+texture with the TV-L1.



(a)



(b)



(c)



(d)

Figure 4-6: (a). Grain Filter for the Cathedral image. Goldstein Synagogue. (b). Gradient Compression. (c). Bilateral filter. (d). Total variation.



(a)



(b)



(c)



(d)

Figure 4-7: Goldstein Synagogue. (a). Nonlocal means (b). Cartoon+Texture (c). Cartoon+texture with the TV-L1. (d). Grain Filter.

5 Conclusions

In this document a comparative study of denoising and geometry/texture decomposition methods for the tone mapping problem was carried out. In the study several classical and new approaches were taken into account. Since it offered a direct path to solve the tone mapping problem, we used the framework developed by Durand et al. They propose to decompose the HDR image in two components, base layer and detail layer. Subsequently, a compression is performed on the base layer and the detail layer added to it. For extracting the base layer they rely on the bilateral filter. Since the goal of bilateral filter in this context is to obtain a smooth image while preserving edges, we use different methods dealing with the same problem, such as, total variation, nonlocal means, cartoon+texture decomposition as in [12] and cartoon+texture using TV-L1. Moreover, we included a filtering method that works specifically with the image level lines allowing the user to remove directly details without corrupting the surroundings, the grain filter as proposed in [32].

From our experimentation, it is easy to conclude how challenging the tone mapping problem is, where there are still some open problems, particularly on: finding a method that is simple to calibrate and with comprehensible parameters, obtaining an ideal balance between illumination, level of detail and robustness to halo artifacts. And although there exist perceptual schemes trying to evaluate tone mapping methods, the most difficult task is to quantize a value that takes multiple meanings from observers and is explicitly the measure of how visually appealing an image is. Without this measure, current methods should rely on tedious parameter tuning process to find the default values that tackle most of the scenes.

In order to avoid this, our study was aimed at identifying the method that presents the most convenient tradeoff. As a result, we concluded that gradient domain compression and bilateral filter offer a practical alternative because a complex tuning of parameters is not necessary. However, they still include halo artifacts and highlight partially detail. Instead, cartoon+texture TV-L1 is efficient at separating the base and detail components and does generate a good balance between parameter tweaking and the visual quality of the resulting image. A second best option is the grain filter considered in the study, but it is important to consider its vulnerability to cause unnatural behaviors.

Bibliography

- [1] Megawave2, 2009. <http://megawave.cmla.ens-cachan.fr/>.
- [2] Ipol journal - Image Processing On Line, 2014. <http://www.ipol.im/>.
- [3] AGUERREBERE, C. *On the Generation of High Dynamic Range Images Theory and Practice from a Statistical Perspective*. PhD thesis, Telecom ParisTech, 2014.
- [4] AGUERREBERE, C., DELON, J., GOUSSEAU, Y., AND MUSÉ, P. Best algorithms for HDR image generation. *A study of performance bounds. HAL-00733853-v2* (2012).
- [5] AUJOL, J.-F., AUBERT, G., BLANC-FÉRAUD, L., AND CHAMBOLLE, A. Image decomposition into a bounded variation component and an oscillating component. *Journal of Mathematical Imaging and Vision* 22, 1 (2005), 71–88.
- [6] BANDO, Y., QIU, G., OKUDA, M., DALY, S., AACH, T., AND AU, O. C. Recent advances in high dynamic range imaging technology. In *Image Processing (ICIP), 2010 17th IEEE International Conference on* (2010), IEEE, pp. 3125–3128.
- [7] BARKOWSKY, M., AND LE CALLET, P. On the perceptual similarity of realistic looking tone mapped high dynamic range images. In *Image Processing (ICIP), 2010 17th IEEE International Conference on* (2010), IEEE, pp. 3245–3248.
- [8] BELL, A., MEYER-EBRECHT, D., BOCKING, A., AND AACH, T. HDR-microscopy of cell specimens: Imaging and image analysis. In *Signals, Systems and Computers, 2007. ACSSC 2007. Conference Record of the Forty-First Asilomar Conference on* (2007), IEEE, pp. 1303–1307.
- [9] BELL, A. A., BRAUERS, J., KAFTAN, J. N., MEYER-EBRECHT, D., BOCKING, A., AND AACH, T. High dynamic range microscopy for cytopathological cancer diagnosis. *Selected Topics in Signal Processing, IEEE Journal of* 3, 1 (2009), 170–184.
- [10] BELL, A. A., KAFTAN, J. N., AACH, T., MEYER-EBRECHT, D., AND BOCKING, A. High dynamic range images as a basis for detection of argyrophilic nucleolar organizer regions under varying stain intensities. In *Image Processing, 2006 IEEE International Conference on* (2006), IEEE, pp. 2541–2544.

- [11] BUADES, A., COLL, B., AND MOREL, J.-M. A non-local algorithm for image denoising. In *Computer Vision and Pattern Recognition, 2005. CVPR 2005. IEEE Computer Society Conference on* (2005), vol. 2, IEEE, pp. 60–65.
- [12] BUADES, A., LE, T., MOREL, J.-M., AND VESE, L. Cartoon+Texture Image Decomposition. *Image Processing On Line 1* (2011). <http://dx.doi.org/10.5201/ipol.2011.blmv.ct>.
- [13] ČADÍK, M., WIMMER, M., NEUMANN, L., AND ARTUSI, A. Evaluation of hdr tone mapping methods using essential perceptual attributes. *Computers & Graphics 32*, 3 (2008), 330–349.
- [14] CHAMBOLLE, A. An algorithm for total variation minimization and applications. *Journal of Mathematical imaging and vision 20*, 1-2 (2004), 89–97.
- [15] CHAMBOLLE, A., AND POCK, T. A first-order primal-dual algorithm for convex problems with applications to imaging. *Journal of Mathematical Imaging and Vision 40*, 1 (2011), 120–145.
- [16] DEBEVEC, P. E., AND MALIK, J. Recovering high dynamic range radiance maps from photographs. In *ACM SIGGRAPH 97* (1997), ACM, pp. 369–378.
- [17] DEMMEL, J. *Solving the Discrete Poisson Equation using Jacobi, SOR, Conjugate Gradients, and the FFT*. U.C. Berkeley, 1996. <http://www.cs.berkeley.edu/~demmell/cs267/lecture24/lecture24.html>.
- [18] DURAND, F., AND DORSEY, J. Fast bilateral filtering for the display of high-dynamic-range images. In *ACM Transactions on Graphics (TOG)* (2002), vol. 21, ACM, pp. 257–266.
- [19] DURAND, F., AND DORSEY, J. *Web miscellany: Fast Bilateral Filtering for the Display of High-Dynamic-Range Images*. MIT - Computer Graphics Group, 2002. <http://people.csail.mit.edu/fredo/PUBLI/Siggraph2002/>.
- [20] DUVAL, V. *Variational and Nonlocal Methods in Image Processing: a Geometric Study*. PhD thesis, Telecom ParisTech, 2011.
- [21] FATTAL, R., LISCHINSKI, D., AND WERMAN, M. Gradient domain high dynamic range compression. In *ACM Transactions on Graphics (TOG)* (2002), vol. 21, ACM, pp. 249–256.
- [22] FERRADANS, S., BERTALMIO, M., PROVENZI, E., AND CASELLES, V. An analysis of visual adaptation and contrast perception for tone mapping. *Pattern Analysis and Machine Intelligence, IEEE Transactions on 33*, 10 (2011), 2002–2012.

- [23] GUEN, V. L. Cartoon+Texture Image Decomposition by the TV-L1 Model. *Image Processing On Line* 4 (2014). <http://dx.doi.org/10.5201/ipol.2014.103>.
- [24] JOBSON, D. J., RAHMAN, Z.-U., AND WOODDELL, G. A. A multiscale retinex for bridging the gap between color images and the human observation of scenes. *Image Processing, IEEE Transactions on* 6, 7 (1997), 965–976.
- [25] JOHNSON, G. M., AND FAIRCHILD, M. D. Rendering HDR images. In *Color and Imaging Conference* (2003), vol. 2003, Society for Imaging Science and Technology, pp. 36–41.
- [26] LIM, B. R., PARK, R.-H., AND KIM, S. High dynamic range for contrast enhancement. *Consumer Electronics, IEEE Transactions on* 52, 4 (2006), 1454–1462.
- [27] LISCHINSKI, D. *HDR Dataset*. The Hebrew University of Jerusalem, <http://www.cs.huji.ac.il/~danix/hdr/results.html>.
- [28] MANTIUK, R., MYSZKOWSKI, K., AND SEIDEL, H.-P. A perceptual framework for contrast processing of high dynamic range images. *ACM Transactions on Applied Perception (TAP)* 3, 3 (2006), 286–308.
- [29] MERTENS, T., KAUTZ, J., AND VAN REETH, F. Exposure fusion. In *Computer Graphics and Applications, 2007. PG'07. 15th Pacific Conference on* (2007), IEEE, pp. 382–390.
- [30] MEYER, Y. *Oscillating patterns in image processing and nonlinear evolution equations: the fifteenth Dean Jacqueline B. Lewis memorial lectures*, vol. 22. American Mathematical Soc., 2001.
- [31] MEYLAN, L. *Tone mapping for high dynamic range images*. PhD thesis, Ecole Polytechnique Federale De Lausanne, 2006.
- [32] MONASSE, P., AND GUICHARD, F. Fast computation of a contrast-invariant image representation. *IEEE Transactions on Image Processing* 9, 5 (2000), 860–872.
- [33] NIKOLOVA, M. Minimizers of cost-functions involving nonsmooth data-fidelity terms. application to the processing of outliers. *SIAM Journal on Numerical Analysis* 40, 3 (2002), 965–994.
- [34] PALMER, S. E. *Vision Science: Photons to Phenomenology*, vol. 1. MIT press Cambridge, MA, 1999.
- [35] PERONA, P., AND MALIK, J. Scale-space and edge detection using anisotropic diffusion. *Pattern Analysis and Machine Intelligence, IEEE Transactions on* 12, 7 (1990), 629–639.

-
- [36] RASKAR, R., AND TUMBLIN., J. Computational photography. <http://web.media.mit.edu/~raskar/photo/>.
 - [37] REINHARD, E., AND DEVLIN, K. Dynamic range reduction inspired by photoreceptor physiology. *Visualization and Computer Graphics, IEEE Transactions on* 11, 1 (2005), 13–24.
 - [38] REINHARD, E., HEIDRICH, W., DEBEVEC, P., PATTANAIK, S., WARD, G., AND MYSZKOWSKI, K. *High dynamic range imaging: acquisition, display, and image-based lighting*. Morgan Kaufmann, 2010.
 - [39] RUDIN, L. I., OSHER, S., AND FATEMI, E. Nonlinear total variation based noise removal algorithms. *Physica D: Nonlinear Phenomena* 60, 1 (1992), 259–268.
 - [40] TOMASI, C., AND MANDUCHI, R. Bilateral filtering for gray and color images. In *Computer Vision, 1998. Sixth International Conference on* (1998), IEEE, pp. 839–846.
 - [41] TUMBLIN, J., AND RUSHMEIER, H. Tone reproduction for realistic images. *Computer Graphics and Applications, IEEE* 13, 6 (1993), 42–48.
 - [42] TUMBLIN, J., AND TURK, G. LCIS: A boundary hierarchy for detail-preserving contrast reduction. In *Proceedings of the 26th annual conference on Computer graphics and interactive techniques* (1999), ACM Press/Addison-Wesley Publishing Co., pp. 83–90.
 - [43] VESE, L. A., AND OSHER, S. J. Modeling textures with total variation minimization and oscillating patterns in image processing. *Journal of Scientific Computing* 19, 1-3 (2003), 553–572.
 - [44] WARD, G. Invited paper: The hopeful future of high dynamic range imaging. In *SID Symposium Digest of Technical Papers* (2007), vol. 38, Wiley Online Library, pp. 1046–1048.